

# Investigation on Turning Inconel 718 Using Nanofluid Under Minimum Quantity Lubrication

Paresh Kulkarni<sup>1</sup>, Satish Chinchankar<sup>1</sup> and Nitin Motgi<sup>2</sup>

<sup>1</sup>Vishwakarma Institute of Information Technology, Pune, Maharashtra, India

<sup>2</sup>Dr. D.Y. Patil Institute of Engineering, Management and Research, Pune, Maharashtra, India

## \*Correspondence to:

Paresh Kulkarni  
Vishwakarma Institute of Information Technology,  
Pune, Maharashtra, India  
E-mail: [paresh.219p0014@viit.ac.in](mailto:paresh.219p0014@viit.ac.in)

Received: January 03, 2024

Accepted: March 15, 2024

Published: March 20, 2024

**Citation:** Kulkarni P, Chinchankar S, Motgi N. 2024. Investigation on Turning Inconel 718 Using Nanofluid Under Minimum Quantity Lubrication. *NanoWorld J* 10(S1): S235-S240.

**Copyright:** © 2024 Kulkarni et al. This is an Open Access article distributed under the terms of the Creative Commons Attribution 4.0 International License (CCBY) (<http://creativecommons.org/licenses/by/4.0/>) which permits commercial use, including reproduction, adaptation, and distribution of the article provided the original author and source are credited.

Published by United Scientific Group

## Abstract

The nickel-based superalloy Inconel 718 is used in aerospace, marine, and defense applications due to its unique qualities. However, these alloys are challenging to cut because of their reduced heat conductivity and propensity for work-hardening. With a focus on sustainability, ongoing efforts are being made to increase the machinability of these alloys. This work investigates the shear angle ( $\phi_n$ ) and chip thickness ratio ( $r$ ) during the turning of Inconel 718 using nanofluid under minimum quantity lubrication (NFMQL) varying cutting speed, feed ( $f$ ), and depth of cut ( $d$ ). Aluminum oxide ( $Al_2O_3$ ) nanoparticles were combined with a 0.25% concentration of commercially available palm oil to create a nanofluid. This study found the closely coiled, serrated continuous chips at higher speeds. The  $r$  and  $\phi_n$  increased with the cutting speed and decreased with the increase in  $f$  and  $d$ . The  $d$  followed by cutting speed and  $f$ , was the most critical parameter for the  $r$  and  $\phi_n$ . This study finds further scope for developing the cutting force model based on the  $r$  and  $\phi_n$  developed models during the oblique turning of Inconel 718 under NFMQL conditions.

## Keywords

Chip thickness ratio, Shear angle, Nanofluid under minimum quantity lubrication, Aluminum oxide, Modelling, Inconel 718

## Introduction

In recent years, numerous attempts were made by researchers towards sustainable manufacturing to stick around to the stringent norms laid down by government authorities to safeguard the environment. The sustainability approach in machining has triggered the usage of various cooling strategies, such as cryogenic cooling, high-pressure jet cooling, minimum quantity lubrication, and NFMQL [1].

Inconel 718 alloy presents divergent challenges during machining in manufacturing industries. Tool wear, power consumption, cutting forces, etc., significantly influences industrial sustainability. Nanoparticle-based cutting fluid has gained advantages in recent years due to their excellent thermo-physical characteristics [2]. Cutting force has a large impact on tool life, surface integrity, dimensional accuracy, and machining power. Knowing it in advance will help in selecting the right machine tool, the cutting insert, and the insert geometry [3].

$\phi_n$  and  $r$  are required to recognize heat generation and deformation during cutting. It is the deciding factor for obtaining the efficiency of chip formation. It has strong relevance with the cutting parameters like an increase in cutting velocity ( $V_c$ ) will decrease the chip thickness and increases the  $r$  [4]. The temperature generated during cutting has a vital importance in the mechanism of chip cre-

ation, this contributes to the cutting tool's thermal deformation, i.e., tool wear [5]. A group of investigators used different nanofluids to machine nickel alloy. Their study suggested the scope for hybrid nanofluids for enhancing cooling and better machinability [6].

Nanoparticle-based cutting fluid is preferred for avoiding the adverse effect of excess heat generation during machining.  $Al_2O_3$ , multi-wall carbon nanotubes, graphene, nanodiamond, silicon oxide, zinc oxide, and a few more nanoparticle-based nanofluids were considered by the researchers under different research works. Nanofluids are formed by mixing them into base fluid with a certain percentage concentration to reach desired properties. The percentage concentration has an important role to play during efficient application at the cutting zone.

While investigating the new bio-based nano-lubricants with varying % concentrations of  $Al_2O_3$  nanoparticles, it was discovered that a 0.8% concentration reduced tool wear and increased tool life due to a generation of favorable spacer attributes. The higher number of nanoparticles could reduce the friction but will cause agglomeration. The agglomeration of nanoparticles increases the coefficient of friction, surface roughness, power expenditure, and specific cutting energy. So, to avoid these adverse effects, 0.5% concentration was found better for machining [7]. Researchers used textured tools with dry and flood cooling to try to machine Inconel 718 [8].

Because Inconel 718 has a history of shear instability and substantial localized deformation at the cutting interface, chip creation is essential in the shearing process. When cutting Inconel 718, a chip with a serrated edge is created. Their creation controls how much tool wear, how much cutting force, and how intact the surface [9]. Material deformation in the case of Inconel 718 is generated by heat softening and/or strain hardening. One of the most important factors in achieving the optimum machinability is the selection of the input cutting parameters. Over  $f$  and  $V_c$ ,  $d$  has the greatest impact on  $\phi_n$  [10]. Shear plane and  $\phi_n$  have vital for cutting dynamics and modeling of the cutting forces. Theoretical cutting force models were developed using  $\phi_n$  theory [11]. A group of researchers attempted modeling  $\phi_n$  and cutting force using the finite element method and findings demonstrated improved agreement with the experimental data [12]. Modelling of  $\phi_n$  using traditional methods such as Merchant, Lee, and Shaffer, and Hucks theories, an attempt was made to link  $\phi_n$  with chip thickness [13]. Attempts were made to extend Waldorf's orthogonal force model to 3D cutting force analysis [14]. To forecast the cutting force, the slip-line field/mechanistic model approach was coupled with the analysis of shear flow stress and  $\phi_n$  [15, 16]. The  $\phi_n$  and  $r$  were found to increase with  $V_c$ . This could be because  $\phi_n$  is direct association with the resultant force [17].

Numerous attempts were made to model the cutting force,  $r$  and  $\phi_n$ . Mathematical models were developed to predict the cutting force considering tool specifications, workpiece properties, process parameters, and cooling conditions. Several attempts were made to develop experimental-based mathematical and numerical models to predict the cutting forces and simulate the cutting mechanism.

In the present scenario of sustainable manufacturing, cutting of Inconel 718 nickel alloy presents certain challenges such as high heat generation, increased cutting forces, and eventually less tool life.  $r$  and  $\phi_n$  are closely associated with metal deformation. Therefore, the development of a reliable model of  $r$  and  $\phi_n$  is key demand to predict and optimize the cutting parameters in the manufacturing industry. The current study presents a model that forecasts the  $r$  and  $\phi_n$  in an oblique cutting process employing a nanofluid-based cutting environment.

## Experimentation

Turning experiments were performed on nickel-based super alloy Inconel 718 bar with a diameter and length of 40 and 400 mm with a hardness of 37 HRC. Physical vapor deposited AlTiN coated tool. The composition of the material has been shown in table 1.

As seen in figure 1, experiments were conducted on a reliable and very accurate CNC lathe. In the study, constant values were maintained for the tool height, tool geometry, and cutting parameters such  $V_c, f, d$  and cutting length. The cutting insert employed had a diamond shape, a nose radius of 0.8 mm and an included angle of  $80^\circ$  as shown in figure 2. Table 2 displays the process parameters that were used in the experiment. To create the nanofluid, 0.25% of  $Al_2O_3$  nanoparticles were added to vegetable-based, commercially available palm oil. The nanofluid was created using a two-step process, as depicted in figure 3.

**Table 1:** Composition (%) of Inconel 718.

C	0.005
Si	0.056
Mn	0.062
P	0.008
S	0.007
Cr	18.37
Mo	2.87
Ni	25.82
Al	0.35
Co	0.22
Nb + Ta	5.01
Ti	1.1
B	0.001
Fe	Balance



**Figure 1:** Experimental setup.

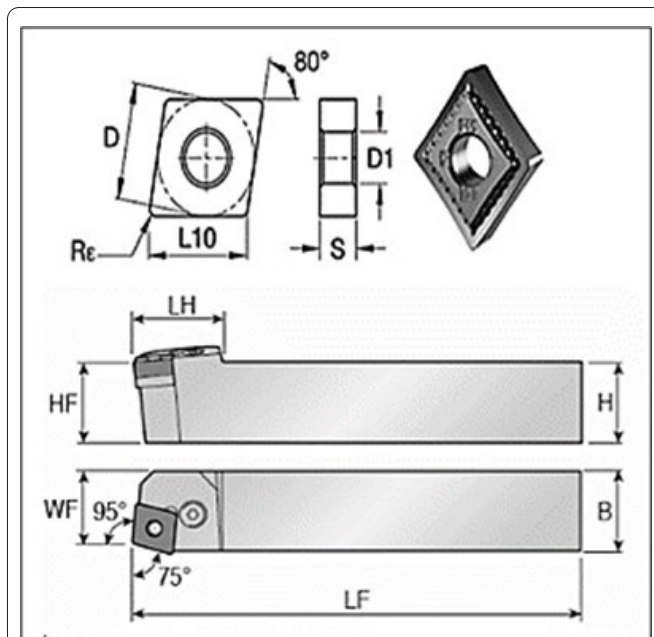


**Figure 2:** Cutting insert (CNMG120408MS) and tool holder (PCBN-R2525M12) geometry.

**Table 2:** Process parameters for turning Inconel 718 under NFMQL.

Process parameters	Values
$V$ (m/min)	30, 45, 65, 85, and 100
$f$ (mm/rev)	0.1, 0.15, 0.2, 0.25, and 0.3
$d$ (mm)	0.2, 0.3, 0.5, 0.7, and 0.8
Tool holder	PCBNR 2525 M12
Cutting insert	PVD-coated AlTiN with geometry CNMG120408MS
MQL flow rate	50 ml/min
Air pressure	4 bar

## Results and Discussion

This section discusses varying the  $r$  and  $\phi_n$  with the cutting parameters by developing a mathematical model during turning Inconel 718 using  $\text{Al}_2\text{O}_3$  NFMQL. The  $r$  and  $\phi_n$  serve an essential role in determining several important response characteristics. A higher  $\phi_n$  will generate thinner chip thickness resulting in an enhanced surface finish and good dimensional accuracy. A lesser chip thickness will help to reduce the temperature generated during cutting which has many positive impacts on machining, such as reduced tool wear, will avoid disturbing the material properties, etc. A higher  $\phi_n$  will suggest a lower shear plane area which tends to have reduced cutting forces and eventually lesser power consumption. Both benefited from manufacturing sustainability.

Table 2 shows the results of fifteen NFMQL turning trials with altering  $V$ ,  $f$ , and  $d$ . Chips were collected after each experiment. The thickness was measured at five different locations using a pre-calibrated digital vernier caliper. An average reading was noted. The cutting tool nomenclature, process parameters, workpiece properties, and cooling conditions significantly affect the machining performance. This study investigates the  $r$  and  $\phi_n$  by developing experimental-based mathematical mod-

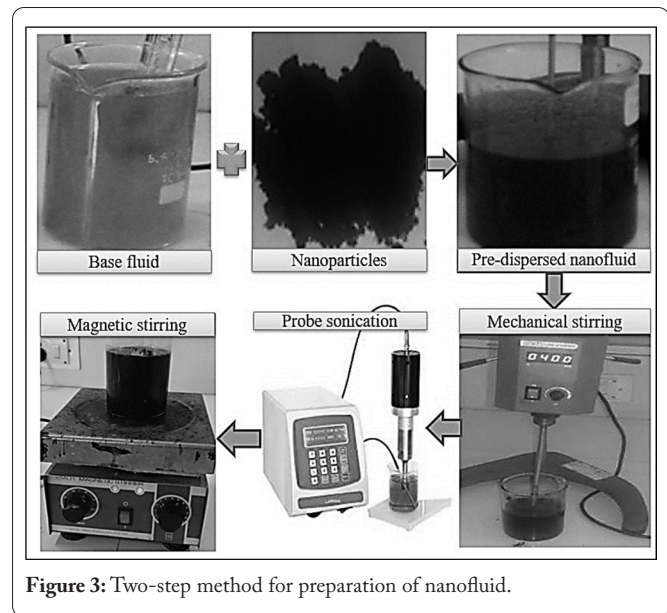


**Figure 3:** Two-step method for preparation of nanofluid.

els. The Chip thickness after cut ( $t_c$ ) and chip thickness before cut ( $t$ ) and  $\phi_n$  are the critical factors to be considered for modeling the  $r$  and  $\phi_n$  in oblique cutting.

In oblique cutting angle from shear plane to the plane containing the newly generated surface of the workpiece measured in a plane normal to the cutting edge will be termed as  $\phi_n$  and is obtained using equation 1.

$$\Phi_n = \tan^{-1} \left( \frac{r \cos \alpha_n}{1 - r \sin \alpha_n} \right) \quad (1)$$

Where ' $\alpha_n$ ' is normal rake angle being of  $-5.96^\circ$  that is obtained using equation 2. The inclination angle ( $i$ ) and the orthogonal rake angle ( $\alpha_o$ ) are referred from the tool manufacturer's catalogue.

$$\tan \alpha_n = \cos i * \tan \alpha_o \quad (2)$$

Where, ' $i$ ' and ' $\alpha_o$ ' which was referred from the manufacturers catalogue. The  $r$  is calculated from equation 3. The  $t$  can be calculated from equation 4.

$$r = \frac{t}{t_c} \quad (3)$$

$$t = f \cos \gamma_s \quad (4)$$

Where ' $f$ ' is feed in mm/rev and ' $\gamma_s$ ' is the side cutting edge angle.

The experimental results were used to create empirical equations. For the  $r$  and  $\phi_n$ , regression equations were created. Using the Data-fit software, the coefficient values in the equation were determined. In equation 5 and equation 6, developed empirical models are presented. All of the created models have R-squared ( $R^2$ ) values that are close to 0.9, which estimate the fraction of variation in the data points. The  $\phi_n$  and  $r$  during turning Inconel 718 using  $\text{Al}_2\text{O}_3$  NFMQL can therefore be precisely predicted by the proposed empirical formulae.

$$r = 0.1618V^{0.1625}f^{-0.1213}d^{-0.4042} \quad (5)$$

$$\phi_n = 10.0936V^{0.1324}f^{-0.104}d^{-0.3179} \quad (6)$$

Two-dimensional plots are drawn by altering the  $V_c$ ,  $f$ , and  $d$  using developed empirical equations. Figure 4a depicts the variation in the  $r$  and  $\phi_n$  with  $V_c$  at  $f$ , and  $d$  of 0.2 mm/rev and 0.5 mm, respectively. The  $r$  and  $\phi_n$  can be seen as increasing with  $V_c$ . An increase in  $\phi_n$  with the  $V_c$  could lower the cutting force. It could be attributed to a reduction in the shear area with the increasing  $\phi_n$  with the  $V_c$ . Moreover, an increase in the  $V_c$  increases the cutting temperature and therefore, makes the material soft and lowers the cutting force. Similarly, a decrease in the shear area lowers the chip thickness and hence increases the chip thickness with the  $V_c$ .

Figure 4b and figure 4c depict the variation in the  $r$  and  $\phi_n$  with the  $f$  and  $d$ , respectively. The  $V_c$  and  $d$  of 65 m/min and 0.5 mm and the  $V_c$  and  $f$  of 65 m/min and 0.2 mm/rev were considered while plotting figure 4b and figure 4c, respectively. The  $r$  and  $\phi_n$  decrease with the  $f$  and  $d$ . A decrease in  $\phi_n$  with the  $f$  could increase the cutting forces. This could be attributed to an increase in the shear area with a decreasing  $\phi_n$  with the  $f$  and  $d$ . An increase in the shear area increases the chip thickness and hence lowers the chip thickness with the  $f$  and  $d$ .

The  $r$  and  $\phi_n$  are prominently affected by the  $d$  followed by the  $f$  and the  $V_c$ . Further, the effect of simultaneously varying the two process parameters on the  $r$  and  $\phi_n$  is plotted using 3D graphs. Figure 5 depicts the 3D plots of the  $r$  varying with the cutting parameters during turning Inconel 718 using  $Al_2O_3$  NFMQL using equation 5.

Figure 5a shows the interaction effect of the  $V_c$  and  $f$  on the  $r$ . The  $r$  can be seen as prominently affected by the  $V_c$  and  $f$ . This could be attributed to a decrease in the chip thickness due to a decrease in the shear plane area and an increase in the cutting temperature with the  $V_c$ . A decrease in the  $r$  can be seen with the increase in the  $f$  and the  $d$  as shown in figure 5b and figure 5c. However, the  $d$  can be seen as significantly affecting the  $r$  than the  $f$  and the  $V_c$ . This is obvious also as the  $t$  increase with the  $d$  and hence the  $r$ .

3D plots showing the  $\phi_n$  varying with the cutting parameters during turning Inconel 718 using  $Al_2O_3$  NFMQL using equation 6 are as shown in figure 6. Figure 6a show the interaction effect of the  $V_c$  and  $f$  on the  $\phi_n$ . The  $\phi_n$  can be seen as increasing with the  $V_c$  and decreasing with the  $f$ . The  $V_c$  can be seen as prominently affecting the  $\phi_n$ . It could be attributed to an increase in the cutting temperature with the  $V_c$  resulting in softening of the workpiece. It lowers the shear plane area and hence the cutting force with the increase in the  $\phi_n$ . On the other hand, a decrease in the  $\phi_n$  can be seen with the increase in  $f$  and the  $d$  from figure 6b and figure 6c. However, the  $d$  can be seen as significantly affecting the  $\phi_n$  than the  $f$ . It could be attributed to rise in the  $t$  and hence the shear plane area with the  $d$ .

Figure 7 shows the images of different sizes and shapes of chips produced varying with cutting parameters during turning Inconel 718 under NFMQL conditions. The chips formed during cutting were serrated continuously coiled helical chips.

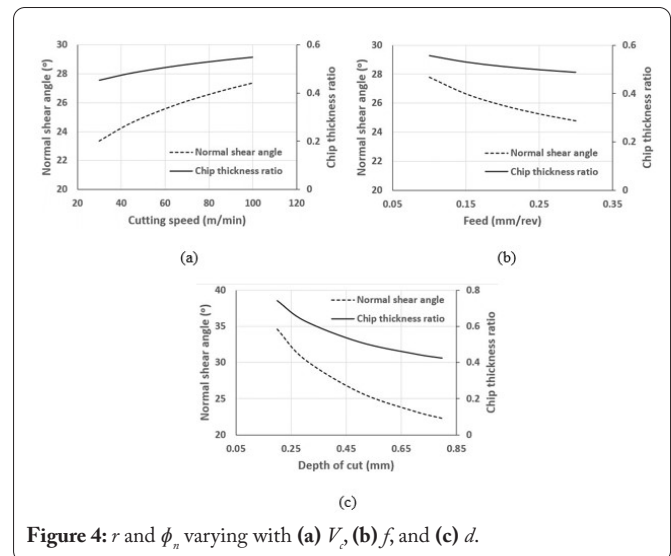


Figure 4:  $r$  and  $\phi_n$  varying with (a)  $V_c$ , (b)  $f$ , and (c)  $d$ .

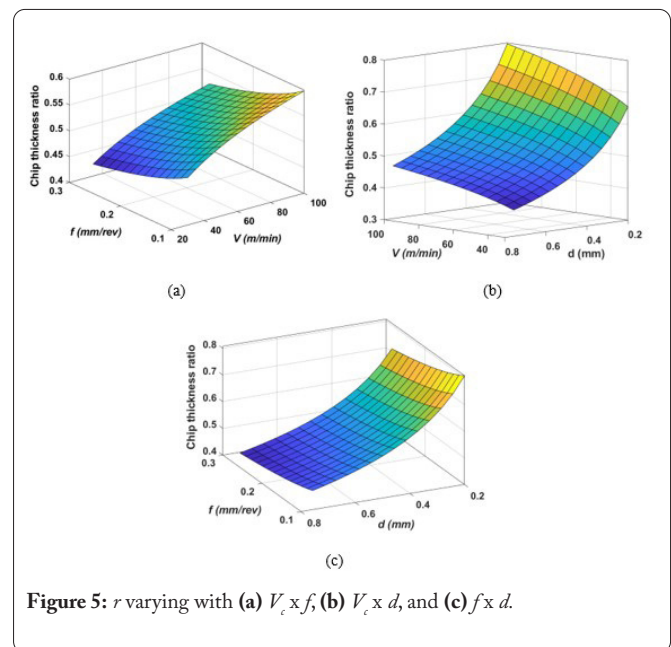


Figure 5:  $r$  varying with (a)  $V_c$  x  $f$ , (b)  $V_c$  x  $d$ , and (c)  $f$  x  $d$ .

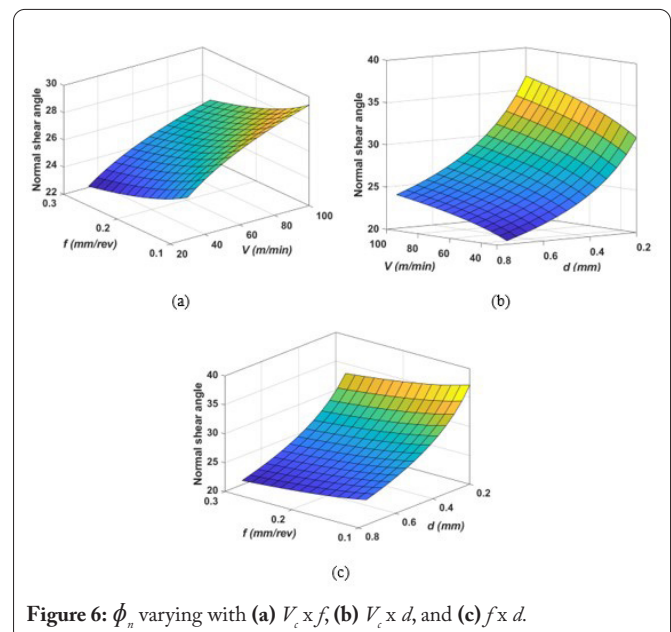


Figure 6:  $\phi_n$  varying with (a)  $V_c$  x  $f$ , (b)  $V_c$  x  $d$ , and (c)  $f$  x  $d$ .

However, the chip with a lower curling radius, i.e., the closely coiled helical chips, were produced at elevated  $V_c$  and  $f$ . And loosely coiled chips (higher curling radius) were produced at lower cutting speeds and  $f$ . It could be attributed to an increase in the frictional coefficient at the chip–tool interface and the cutting temperature with the  $V_c$  resulting in a higher temperature variance between the chip's free and sliding surfaces.

This study finds that  $r$  and  $\phi_n$  are significantly affected by the  $d$  followed by the  $V_c$  and  $f$ . The coefficient of determination for the developed mathematical models was close to 0.9, showing that the generated models could be reliably used to forecast the  $r$  and  $\phi_n$  within the boundaries of the process parameters considered for this investigation. Predicted R-squared values were in close agreement with adjusted R-squared values showing that models do not appear to overfit and possess sufficient predictability for the  $r$  and  $\phi_n$ . This study finds further scope for developing cutting force models based on the developed models for the  $r$  and  $\phi_n$  during oblique turning of Inconel 718 under NFMQL conditions.

Additionally, the study suggests that future research should focus on investigating the effects of different cutting parameters on the surface roughness and tool wear during oblique turning of Inconel 718. Furthermore, understanding the relationship between the  $r$  and  $\phi_n$  could provide valuable insights for optimizing machining processes to improve productivity and reduce costs.

## Conclusions

This study investigated the  $r$  and  $\phi_n$  during turning Inconel 718 using NFMQL. The mathematical models were developed with the goal to gain a deeper comprehension of how the process factors affect chip thickness and  $\phi_n$ . Commercially available vegetable palm oil was used as a base fluid. A nanofluid was prepared by mixing  $Al_2O_3$  nanoparticles in palm oil with 0.25% concentration. The current investigation could lead to the following conclusions:

- The  $r$  and  $\phi_n$  were increased with the  $V_c$  and decreased with the increase in  $f$  and  $d$ . However, the  $r$  and  $\phi_n$  were prominently affected with the  $d$ .
- An increase in the  $r$  with the  $V_c$  could be attributed to a decrease in the chip thickness and hence the shear plane area and an increase in the cutting temperature with the  $V_c$ . On the other hand, decreasing the  $r$  with the  $f$  and  $d$  could be attributed to an increase in the  $t$  with the  $f$  and the  $d$ .
- An increase in the  $\phi_n$  with the  $V_c$  could be attributed to an increase in the cutting temperature with the  $V_c$  resulting in softening of the workpiece. It lowers the shear plane area and hence the cutting force. However, a decrease in the  $\phi_n$  with the  $f$  and  $d$  could be attributed to an increase in the uncut chip thickness and hence the shear plane area with the  $f$  and  $d$ .
- The coefficient of determination for the created mathematical models was close to 0.9, suggesting that the models could be used to forecast the  $r$  and  $\phi_n$  within the scope of the current study's process parameters.

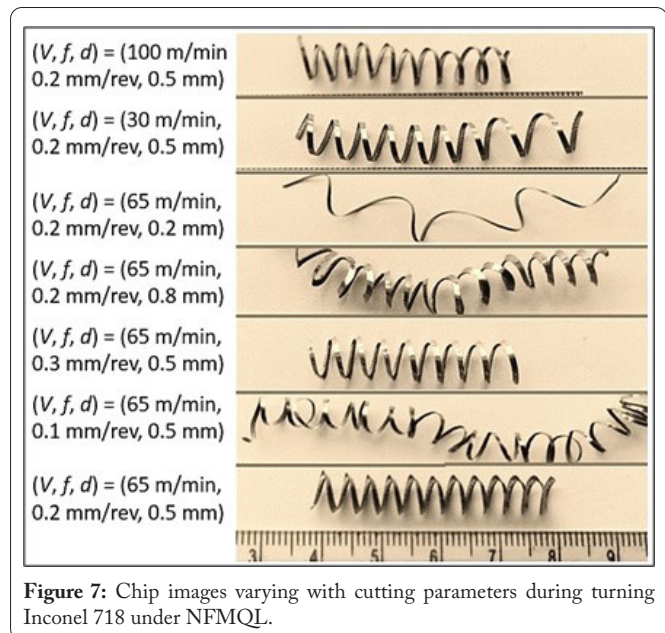


Figure 7: Chip images varying with cutting parameters during turning Inconel 718 under NFMQL.

- Serrated continuously coiled helical chips were produced at elevated  $V_c$  and  $f$ . It could be attributed to a higher temperature variance between the chip's free and sliding surfaces at higher cutting speeds.

## Acknowledgments

None.

## Conflict of Interest

None.

## References

1. Khanna N, Agrawal C, Dogra M, Pruncu CI. 2020. Evaluation of tool wear, energy consumption, and surface roughness during turning of Inconel 718 using sustainable machining technique. *J Mater Res Technol* 9(3): 5794-5804. <https://doi.org/10.1016/j.jmrt.2020.03.104>
2. Chinchani S, Kore SS, Hujare P. 2021. A review on nanofluids in minimum quantity lubrication machining. *J Manuf Process* 68: 56-70. <https://doi.org/10.1016/j.jmapro.2021.05.028>
3. Orra K, Choudhury SK. 2018. Mechanistic modelling for predicting cutting forces in machining considering effect of tool nose radius on chip formation and tool wear land. *Int J Mech Sci* 142: 255-268. <https://doi.org/10.1016/j.ijmecsci.2018.05.004>
4. Thamizhmanii S, Sulaiman H. 2012. Machinability study using chip thickness ratio on difficult to cut metals by CBN cutting tool. *Key Eng Mater* 504: 1317-1322. <https://doi.org/10.4028/www.scientific.net/KEM.504-506.1317>
5. Abukhshim NA, Mativenga PT, Sheikh MA. 2005. Investigation of heat partition in high-speed turning of high strength alloy steel. *Int J Mach Tools Manuf* 45(15): 1687-1695. <https://doi.org/10.1016/j.ijmachtools.2005.03.008>
6. Kulkarni P, Chinchani S. 2023. A review on machining of nickel-based superalloys using nanofluids under minimum quantity lubrication (NFMQL). *J Inst Eng India Ser C* 104: 183-199. <https://doi.org/10.1007/s40032-022-00905-w>
7. Ali MA, Azmi AI, Murad MN, Zain MZ, Khalil AN, et al. 2020. Roles of new bio-based nanolubricants towards eco-friendly and improved machinability of Inconel 718 alloys. *Tribol Int* 144: 106106. <https://doi.org/10.1016/j.triboint.2019.106106>

8. Rajurkar A, Chinchani S. 2022. Experimental investigation on laser-processed micro-dimple and micro-channel textured tools during turning of Inconel 718 alloy. *J Mater Eng Perform* 31: 4068-4083. <https://doi.org/10.1007/s11665-021-06493-7>
9. Pawade RS, Joshi SS. 2011. Mechanism of chip formation in high-speed turning of Inconel 718. *Mach Sci Technol* 15(1): 132-152. <https://doi.org/10.1080/10910344.2011.557974>
10. Ramana MV, Rao GK, Prasanth G, Sagar B, Kumar PR, et al. 2021. Effect of machining conditions on shear angle in turning of A286 iron based nickel super alloy. *Mater Today Proc* 44: 2319-2324. <https://doi.org/10.1016/j.matpr.2020.12.407>
11. Berezvai S, Molnar TG, Bachrathy D, Stepan G. 2018. Experimental investigation of the shear angle variation during orthogonal cutting. *Mater Today Proc* 5(13): 26495-26500. <https://doi.org/10.1016/j.matpr.2018.08.105>
12. Lee WB, Wang H, Chan CY, To S. 2013. Finite element modelling of shear angle and cutting force variation induced by material anisotropy in ultra-precision diamond turning. *Int J Mach Tools Manuf* 75: 82-86. <https://doi.org/10.1016/j.ijmachtools.2013.09.007>
13. Hao M, Xu D, Feng P. 2019. Numerical and experimental investigation of the shear angle in high-speed cutting of Al6061-T6. *Int J Adv Manuf Technol* 100: 3037-3044. <https://doi.org/10.1007/s00170-018-2842-8>
14. Chinchani S, Choudhury SK. 2016. Cutting force modeling considering tool wear effect during turning of hardened AISI 4340 alloy steel using multi-layer TiCN/Al<sub>2</sub>O<sub>3</sub>/TiN-coated carbide tools. *Int J Adv Manuf Technol* 83: 1749-1762. <https://doi.org/10.1007/s00170-015-7662-5>
15. Smithey DW, Kapoor SG, DeVor RE. 2001. A new mechanistic model for predicting worn tool cutting forces. *Mach Sci Technol* 5(1): 23-42. <https://doi.org/10.1081/MST-100103176>
16. Waldorf DJ, DeVor RE, Kapoor SG. 1997. A slip-line field for ploughing during orthogonal cutting. *J Manuf Sci Eng* 120(4): 693-699. <https://doi.org/10.1115/1.2830208>
17. Tang L, Huang J, Xie L. 2011. Finite element modeling and simulation in dry hard orthogonal cutting AISI D2 tool steel with CBN cutting tool. *Int J Adv Manuf Technol* 53: 1167-1181. <https://doi.org/10.1007/s00170-010-2901-2>